Cell and Tissue Research (2019) 375:709–721
https://doi.org/10.1007/s00441-018-2927-6

REGULAR ARTICLE

Nanofiber-acellular dermal matrix as a bilayer scaffold containing mesenchymal stem cell for healing of full-thickness skin wounds

Mohamad Javad Mirzaei-parsa[1] · Hossein Ghanbari[1] · Behnam Alipoor[2] · Amirhossein Tavakoli[3] · Mohammad Reza H. Najafabadi[1] · Reza Faridi-Majidi[1]

Received: 15 March 2018 / Accepted: 18 September 2018 / Published online: 18 October 2018

Abstract

Full-thickness skin defect is one of the main clinical problems, which cannot be repaired spontaneously. The aim of this study was to evaluate the feasibility of combining nanofibers with ADM as a bilayer scaffold for treatment of full-thickness skin wounds in a single-step procedure. The nanofibrous polycaprolactone/fibrinogen scaffolds were fabricated by electrospinning. Subsequently, mesenchymal stem cells were isolated from rat adipose tissues and characterized by flow cytometry. Cell adhesion, proliferation, and the epidermal differentiation potential of adipose-derived stem cells (ADSCs) on nanofibrous scaffolds were investigated by scanning electron microscopy (SEM), alamarBlue, and real-time PCR, respectively. In animal studies, full-thickness excisional wounds were created on the back of rats and treated with following groups: ADM, ADM-ADSCs, nanofiber, nanofiber-ADSCs, bilayer, and bilayer-ADSCs. In all groups, wounds were harvested on days 14 and 21 after treatment to evaluate re-epithelialization, blood vessel density, and collagen content. The results indicated that ADSCs seeded on ADM, nanofiber, and bilayer scaffolds can promote re-epithelialization, angiogenesis, and collagen remodeling in comparison with cell-free scaffolds. In conclusion, nanofiber-ADSCs showed the best results for re-epithelialization (according to histological scoring), average blood vessel density (92.7 ± 6.8), and collagen density (87.4 ± 4.9%) when compared to the control and other experimental groups.

Keywords Nanofiber scaffold · Acellular dermal matrix · Adipose-derived stem cells · Wound healing · Tissue engineering

✉ Reza Faridi-Majidi
refaridi@sina.tums.ac.ir

Mohamad Javad Mirzaei-parsa
m_parsa@razi.tums.ac.ir

Hossein Ghanbari
hghanbari@tums.ac.ir

Behnam Alipoor
behnam.alipour@yums.ac.ir

Amirhossein Tavakoli
amirtavakoli1@yahoo.com

Mohammad Reza H. Najafabadi
hasani.njf@gmail.com

[1] Department of Medical Nanotechnology, School of Advanced Medical Technologies, Tehran University of Medical Sciences, Tehran, Iran

[2] Department of Laboratory Sciences, Faculty of Paramedicine, Yasuj University of Medical Sciences, Yasuj, Iran

[3] Iranian Tissue Bank Research Centre, Tehran University of Medical Sciences, Tehran, Iran

Introduction

Full-thickness skin wounds caused by various kinds of injuries, such as acute trauma, chronic ulcers, and extensive burns develop many physiological and functional problems (Wang et al. 2015). In full-thickness wounds when both epidermis and dermis are lost, the skin cannot regenerate spontaneously (Ma et al. 2011). The standard treatment for wound coverage is thin split-thickness skin autografts (Wang et al. 2013). However, the scar formation and donor site availability are the main disadvantages of split-thickness skin (Foubert et al. 2015; Ryssel et al. 2008). Thus, to reduce scar contraction and improve the quality of the grafted area, the application of dermal substitutes is a suitable option (Haslik et al. 2010). Normally, in a two-step procedure, the dermal substitutes are covered by an autologous split-thickness skin graft after 21 days (Philandrianos et al. 2012). This delay in two-step procedures is essential for the integration of the matrix and sufficient ingrowth of the vasculature into the dermal substitute to avoid autograft loss (Philandrianos et al. 2012; Wang et al. 2013). The main disadvantage of this method is the

relatively long time of healing and unnecessary secondary operations. Therefore, a simple one-step procedure was proposed to decrease the time to heal and improve the outcome (Wang et al. 2013; Wood et al. 2007). In the one-step procedure, the dermal substitute and a split-thickness skin graft were simultaneously used in one operation to close the wounds (Wang et al. 2013). Numerous studies have used acellular dermal matrix (ADM), Integra, or Matriderm covered by an autologous split-thickness skin graft in a one-step procedure (Demiri et al. 2013; Ryssel et al. 2008; Soejima et al. 2006; Wang et al. 2013; Wood et al. 2007). However, there is no study evaluating the feasibility of nanofiber as an alternative for split-thickness graft. Electrospun nanofibers have been widely used as tissue engineering scaffold due to the similarity of structure to the natural extracellular matrix (ECM) (Mirzaei et al. 2016). Nanofibrous scaffolds have been presented as a suitable substrate for tissue engineering of damaged skin since they offer some advantages, such as possessing high surface area-to-volume ratio, promoting cell proliferation, and removal of exudates from the wound bed (Hosseinzadeh et al. 2017; Sundaramurthi et al. 2014). Stem cell-based therapy is another approach to improve skin regeneration in cutaneous wounds (Wang et al. 2015). Adipose-derived stem cells (ADSCs) are known to significantly decrease the wound size and accelerate the re-epithelialization process (Jin et al. 2013). Accordingly, in the current study, ADM was covered by a layer of nanofiber containing ADSCs to treat full-thickness skin defects. Moreover, the effectiveness of ADM and nanofiber scaffold with or without ADSCs were evaluated in full-thickness wound healing.

Material and methods

Fabrication of nanofibers

The nanofibrous scaffolds were prepared and characterized according to our previous study. Briefly, polycaprolactone (PCL) and fibrinogen (Fbg) were dissolved at a ratio of 50:50 (wt%) in nine parts 1,1,1,3,3,3-hexafluoroisopropanol (HFIP; Hangzhou Dingyan, China) and one part Dulbecco's modified Eagle medium (DMEM, Inoclon, Iran) to obtain 10% (*w*/*v*) solution. The electrospinning process was performed using electrospinning equipment (Electroris, FNM, Tehran, Iran). The prepared solution was filled in a 5-ml syringe attached to a blunt steel needle at a flow rate of 1.0 ml/h with a high voltage of 20 kV. The distance was set for 12 cm from the needle tip.

Preparation of ADM

ADM from rat was prepared by Iranian Tissue Bank & Research Center (Imam Khomeini Hospital, Tehran, Iran).

Preparation of bilayer scaffolds

For bilayer scaffolds, the nanofibers were attached to ADM with collagen solution (2 wt%). After freeze-drying, the bilayer scaffolds fixed with absorbable surgical sutures for in vivo transplantation.

Isolation and culture of ADSCs

Mesenchymal stem cells (MSCs) were isolated from adipose tissue of Wistar rats. Briefly, adipose tissue was harvested and washed three times with PBS and 2% antibiotics (Pen/Step, Gibco) then chopped in a sterile tissue culture plate (TCP). This tissue was digested in a collagenase type I (1 mg/ml, Invitrogen) for 40 min, at 37 °C. After incubation, DMEM/F12 containing 10% FBS (Gibco) was added to stop the enzymes' activity followed by filtrations using 70-μm cell strainer. The suspension centrifuged at 200 ×*g* for 5 min and the cell pellet was re-suspended in erythrocyte lysing buffer (160-mM NH4Cl) for 10 min at room temperature. Finally, the cell pellet was re-suspended in DMEM/F12 medium supplemented with 10% FBS and 1% P/S and kept at 37 °C under 5% CO_2. After 48 h, the culture media were replaced to remove non-adhered cells.

Stem cell characterization

MSCs were characterized by flow cytometry after three cell passages. The antibodies used were as follows: PerCP/Cy5.5 anti-rat CD90.1 (Biolegend), FITC anti-rat CD45.2, FITC anti-rat CD44H (Biolegend), purified mouse anti-rat CD73, and PE rat anti-mouse IgG1 supplied from BD PharMingen. Cells were incubated for 30 min and analyzed by FACSCalibur (BD Biosciences) flow cytometer. Subsequently, acquired data were analyzed by utilizing the Flowjo7.6 software.

Culture of ADSCs on the scaffolds

Electrospun nanofibrous scaffolds was cut out with a punch, sterilized by gamma irradiation (25 kGy), and then placed in a 24-well culture plate (Nunc, Denmark). The cells in cell culture flasks were harvested by treating with 0.25% trypsin-EDTA (Invitrogen, USA) and seeded at a density of 6000 cells/well.

Differentiation of ADSCs toward the epidermal lineage

The stem cells were seeded on the PCL/Fbg scaffolds in a 24-well plate using DMEM/F12 medium supplemented with FBS (5%), 1× insulin–transferrin–selenium (ITS, Sigma), 0.5-μg/ml hydrocortisone (Sigma), 10-ng/ml epithelial

growth factor (EGF, Peprotech), 10-ng/ml keratinocyte growth factor (KGF, Peprotech), and 50-μg/ml L-ascorbic acid (Sigma). The induction medium was changed every 2 days and continued for 9 days.

Morphology of differentiated and undifferentiated ADSCs

The morphology of ADSCs on the nanofibrous scaffolds was investigated using normal growth and epidermal induction media at the end of 6 and 9 days, respectively, by SEM. The cell-scaffold constructs were washed with PBS and fixed with Karnovsky's fixative (2% paraformaldehyde, 2.5% glutaraldehyde) for 30 min, followed by washing with deionized water. They were then dehydrated through a graded series of ethanol solutions (30, 50, 70, 90, and 100%) for 5 min and allowed to dry on a clean petri dish. Finally, the samples were observed by SEM (Philips XL-30) after sputter-coated with gold.

Cell viability and proliferation

The viability and proliferation of ADSCs on the nanofibrous scaffolds and TCP as a control were investigated using alamarBlue reagent reduction assay. At time points of 1, 3, and 7 days, medium on the cell-seeded scaffolds was removed and replaced with alamarBlue working solution (10%, Invitrogen, USA) and then incubated for 3 h at 37 °C. Then 100 μl of solution from each well was transferred into a 96-well plate. The absorbance was measured at 570 and 600 nm using a microplate reader. Results are presented as mean ± standard deviation of experiments performed in triplicate.

Real-time PCR

The stem cells were seeded at a density of 6×10^3 on nanofibrous scaffolds in a 24-well plate for 9 days. Total cellular RNA was extracted using RNX—Plus kit (Sinaclon, Iran). The isolated RNA was quantified using a NanoDrop spectrophotometer (Thermo Scientific). RNA samples were reversely transcribed to obtain complementary DNA (cDNA) using primescript™ RT Reagent kit (Takara Bio, Inc.) according to the manufacturer's recommendations. All specific primers sets for studied genes including keratin 10 (Krt 10), filaggrin (Flg), involucrin (Ivl), and also glyceraldehyde 3-phosphate dehydrogenase (GAPDH) as internal control were listed in Table 1. The PCR was performed in triplicate according to the standard program: 95 °C for 6 min, 40 cycles of 95 °C for 40 s, 63 °C for 40 s, and 72 °C for 35 s and a final extension step of 72 °C for 10 min. All the melting curves contain single peaks, conforming specific PCR amplification. After evaluating the PCR efficiency by LinReg PCR software, the relative expression levels were measured by $2^{-\Delta\Delta ct}$ method.

Preparing ADSC-loaded scaffolds for in vivo transplantation

Pieces of ADM and nanofibrous scaffolds with the average thickness of 350 ± 100 and 160 ± 50 μm, respectively, were placed in 12-well TCP and seeded with ADSCs at a density of 3×10^5/well. Then the plate was kept in a 37 °C with 5% CO_2. After 48 h, the cell-scaffolds were ready to transfer and sutures on the wound of rats.

Wound model and scaffolds implantation

Fifty-six Wistar rats weighing 180 ± 20 g were used in this study. Animals were anesthetized with an intraperitoneal injection of ketamine (50 mg/kg) and xylazine (10 mg/kg), shaved, and sterilized with iodine and ethanol 70% prior to surgery. A full-thickness wound of 2 cm × 2 cm was created with scissors on the back of each animal. The wounded rats were divided into the following seven groups. (a) Control (no graft), (b) ADM, (c) ADM containing ADSCs, (d) nanofiber, (e) nanofiber containing ADSCs, (f) bilayer scaffold, and (g) bilayer scaffold containing ADSCs (each group consisting of eight animals). Each group is divided into 14 and 21 days. All animal experiments were approved by the local Animal Care Committee of Tehran University of Medical Sciences.

Histopathological study

Four animals from each group were euthanized 14 and 21 days post-treatment, and the skin tissues were harvested and immediately fixed in the 10% neutral buffered formalin (pH 7.26) for 48 h. Then the fixed tissue samples were processed, embedded in paraffin, and sectioned to 5-μm thickness. Finally, the sections were stained with hematoxylin and eosin (H&E) and Masson's trichrome (MT). The histological slides were evaluated by the independent reviewer, using light microscopy (Olympus BX51; Olympus, Tokyo, Japan). Epithelialization, inflammatory cell infiltration, fibroplasia, and granulation tissue formation have been assessed in different groups, comparatively.

Immunohistochemical analysis

CD31 immunohistochemical staining was performed in order to investigate the angiogenesis during wound healing process. To do so, tissue sections from the injured area were analyzed for expression of the following primary antibodies: CD31 (ab119339, Abcam, MA, USA). For heat-induced epitope retrieval (HIER), the slides were incubated in citrate buffer (Dako, Glostrup, Denmark) solution at 60 °C overnight. The

Table 1 Forward and reverse primers sequences used for real-time PCR

Gene	Sequence (5 → 3′)	Primer length	Tm	Product length
Krt 10	F-AAGGTGACCATGCAGAACCT	20	59.23	117
	R-GTGCTTCTCGTACCACTCCT	20	59.111	
Flg	F-GCCACTCCGACTACTCAGAA	20	58.83	147
	R-CGTCCTCGGTTTCTTCTACAC	21	58.41	
Ivl	F-CAGGAGCTGGATGACTCACA	20	59.10	122
	R-GTCAGGTTCTCCAATTTGTG CT	22	59.11	
Gapdh	F-CCATCACTGCCACTCAGAAG	20	58.26	136
	R-TTCAGCTCTGGGATGACCTT	20	58.34	

slides were then blocked with 1% hydrogen peroxide/methanol (Sigma-Aldrich, St. Louis, MO, USA) at RT for 30 min, followed by an overnight incubation with primary antibodies at 4 °C. The color reaction was developed with ready to use 3,3′-diaminobenzidine (Dako liquid DAB color solution), and the slides were then counterstained with hematoxylin.

Histomorphometry analysis

Epithelialization in day 21 was assessed semiquantitatively on 5 point scale: 0 (without new epithelialization), 1 (25%), 2 (50%), 3 (75%), and 4 (100%). For these parameters, results were validated by comparative analysis of one independent observer blinded to the treatment groups. In addition, for histomorphometric analysis, neovascularization and collagen density were calculated and analyzed, using computer software Image-Pro Plus® V.6 (Media Cybernetics, Inc., Silver Spring, USA).

Statistical analysis

Statistical analyses were performed using the SPSS software, version 20.0 (SPSS, Inc., Chicago, USA). Normality test was done by the Shapiro-Wilk test. The groups were compared by student's *t*-test for the normally distributed data or Mann-Whitney *U* test for the nonparametric data. ANOVA and Kruskal-Wallis tests were used for the comparisons of quantitative variables between three or more groups, depending on whether the data were normally distributed. Results with *P* values of less than 0.05 were considered statistically significant.

Results

ADSC characterization

Flow cytometry analysis was performed in order to detect the surface markers of ADSCs. As shown in Fig. 1, the results show that cells were negative for the marker of hematopoietic cells (CD45) and strongly expressed CD44 (100%), CD73 (98.5%) and CD90 (100%).

Proliferation of ADSCs on the electrospun nanofibrous scaffolds

The viability and proliferation capacity of ADSCs on nanofibrous scaffolds was determined using alamarBlue assay. According to the results, there is a significant difference in the cell proliferation between PCL and PCL/Fbg except for the first day. On days 3 and 7, the cell proliferation on PCL/Fbg showed enhanced proliferation compared with cells cultured on PCL nanofibers ($P < 0.05$). On day 7, the percentage reduction of alamarBlue reagent, which is proportional to the cell viability and proliferation of ADSCs on the electrospun nanofibrous, was 88 ± 2.8 and $98 \pm 5.6\%$ for PCL and PCL/Fbg, respectively (Fig. 2).

Morphology of differentiated ADSCs into epidermal lineage

The morphology of differentiated ADSCs toward epidermal lineage was studied on TCP and nanofibrous scaffolds. The spindle-shaped, fibroblastic morphology of undifferentiated ADSCs (Xu et al. 2008) can be observed in Fig. 3a, b. However, when ADSCs were exposed to epidermal induction medium containing EGF, KGF, ITS, hydrocortisone, and L-ascorbic acid, the phenotypical features of stem cells were changed into polygonal or round morphologies (Fig. 3c, d). The normal human epidermal keratinocytes (NHEK, Lonza) was used as positive control. As shown in Fig. 3e, f, NHEK cells have round morphologies.

Real-time PCR

To confirm the epidermal differentiation of ADSCs cultured on the nanofibrous scaffold with induction media, RT-PCR analysis was used to evaluate the expression of specific markers for keratinocytes, such as Krt 10, Flg, and Ivl after

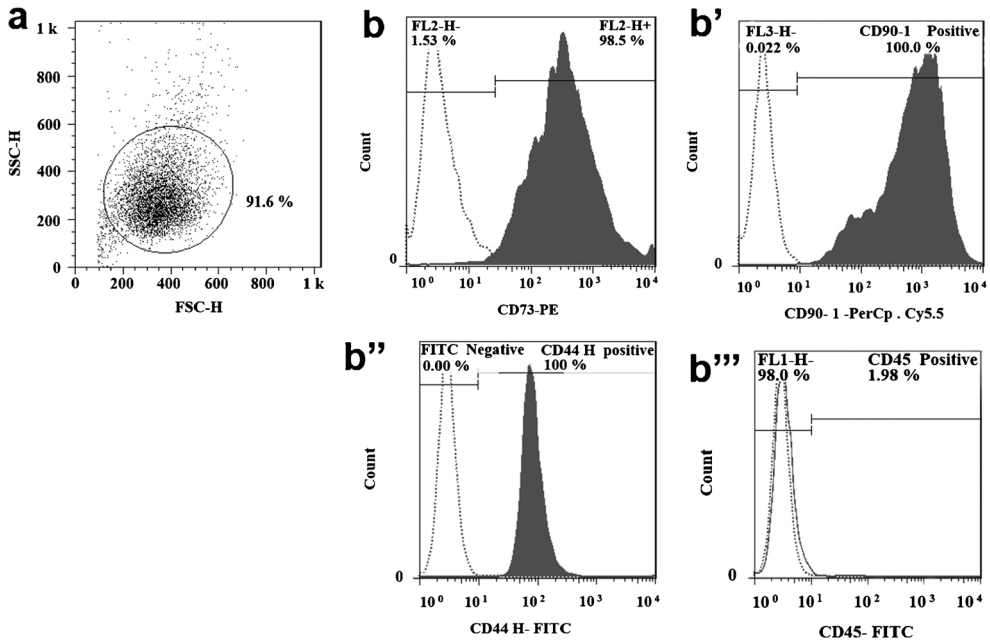

Fig. 1 Flow cytometric analysis of the isolated adipose-derived stem cells. **a** The cells were gated for stem cells (FSC-H vs SSC-H) and then were analyzed for expression of surface markers. The cells were positive for CD73 b, CD90 b′, CD44 b″, and they were negative for CD45 b‴ which is demonstrated the presence of mesenchymal stem cells. The gray peaks represent the cell surface staining with fluorescent-conjugated antibodies; the white peaks represent the unstained cells

9 days of cell seeding. Undifferentiated cultured ADSCs on nanofibrous scaffolds were considered as the control group. Our results revealed that the expression levels of Krt10, Flg, and Ivl in differentiated cells were approximately 2.52-, 2.17-, and 9.22-fold higher in comparison to the control group ($P < 0.05$) (Fig. 4).

Gross wound observation

Gross wound observation was performed to investigate the wound closure rate and wound healing. The appearance of wound site in different groups (control, ADM, ADM-ADSCs, nanofiber, nanofiber-ADSCs, bilayer, and bilayer-ADSCs) was shown in Fig. 5. In some groups, the surrounding hair was re-shaved to show the wound margin clearly. Re-epithelialization had progressed well in wounds treated with nanofiber-ADSCs and bilayer-ADSCs in comparison with the other groups. In the control group even on day 21, the wounds were little re-epithelialized and not fully closed. By the day 21, significant differences were observed among all experimental and control groups ($P < 0.05$). The wound closure rate for ADM, nanofiber, and bilayer were 75 ± 3, 87 ± 1.6, and 80 ± 1.7%, respectively. However, when the ADSCs seeded onto these scaffolds, the wound areas decreased and the healing process was significantly accelerated and reached to 83 ± 2.9, 96 ± 2, and 90 ± 1.4%, respectively (the curve for wound closure rate is shown in Fig. 6).

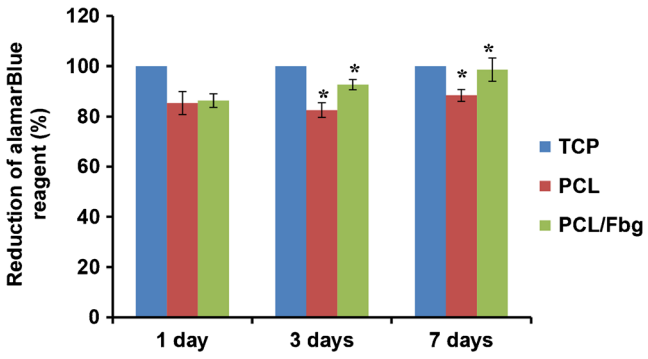

Fig. 2 Proliferation of ADSCs on PCL/Fbg nanofibrous in comparison with PCL by using alamarBlue assay on days 1, 3, and 7. Data are presented as mean ± SD, $n = 3$ (*$P < 0.05$). Abbreviations: PCL (polycaprolactone), Fbg (fibrinogen), TCP (tissue culture plate)

Histological analysis

Histological analysis of the skin wounds was performed by H&E staining as it is shown in Fig. 7. In control group, the wounds were left without any treatment and the histopathological evaluation of this group at 14 and 21 days post-treatment showed polymorphonuclear inflammatory cell (PMN) infiltration and granulation tissue formation; however, the epidermal layer has not been formed and the wound was covered by a crusty scab. Histopathological evaluation of ADM group at day 14 revealed a close similarity with the control group; a crusty scab covered the wound area without epidermal formation and the presence of inflammation in wound area was evident. On day 21, although a narrow layer of epithelial cells was formed, inflammation was evident in defect site and the number of inflammatory cells decreased compared to the control group at the same time. Micrographs of the ADM-ADSCs group at 14 and 21 days post-treatment showed severe infiltration of inflammatory cells into defect area; however, the number of inflammatory

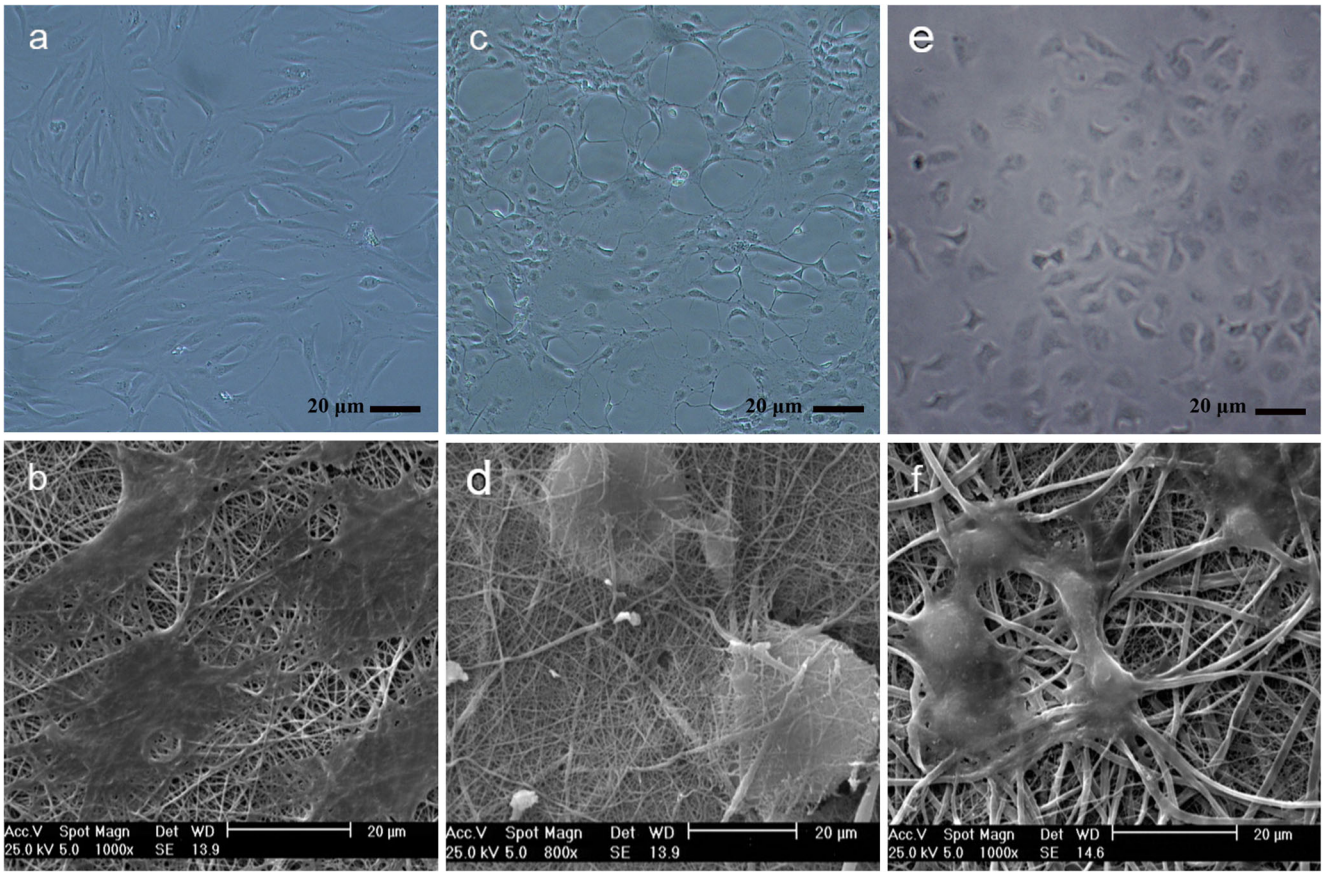

Fig. 3 The morphology of ADSCs, epidermally differentiated ADSCs, and NHEK cells on TCP and electrospun nanofibrous scaffolds. Morphology of ADSCs on TCP (**a**) and on nanofibrous scaffold (**b**). Morphology of epidermally differentiated ADSCs on TCP (**c**) and on nanofibrous scaffold (**d**). Morphology of NHEK cells on TCP (**e**) and on nanofiber scaffold (**f**). Abbreviations: NHEK (normal human epidermal keratinocytes), ADSCs (adipose-derived stem cells), TCP (tissue culture plate)

cells decreased when compared to ADM group. On day 21, epidermis and dermis started to form. The rejuvenation of hair follicles was also evident in this group at 21 days post-treatment. Histopathology of wounds treated by nanofiber scaffolds showed epidermal proliferation and increasing the epidermal layer at 14 days post-treatment. The inflammatory response and granulation tissue were gradually decreased during 21 days of treatment with this scaffold. Micrographs of this group showed the rejuvenation of the other skin appendages, such as sebaceous glands. Histopathological evaluation of nanofiber-ADSCs showed a considerable inflammation reduction at day 14 in comparison to the others. This group showed more resemblance to normal skin, with a thin epidermis and presence of normal rete ridges, and normal thickness of skin layers. Micrographs of the bilayer group at 14 days post-treatment showed the granulation tissue characterized by neovascularization in a background of inflammatory cell infiltration and fibroplasia. On day 21, wounds in this group demonstrated epithelialization without regeneration of skin appendages. Histopathological evaluation of bilayer-ADSCs group showed a considerable inflammation reduction at day 14 in comparison to the cell-free bilayer group. The hair follicles and other skin appendages were also regenerated in this group at 21 days post-treatment. Overall, the results indicate that the scaffold incorporated with ADSCs leads to inflammation reduction and better re-epithelialization when compared to control and other cell-free scaffold groups.

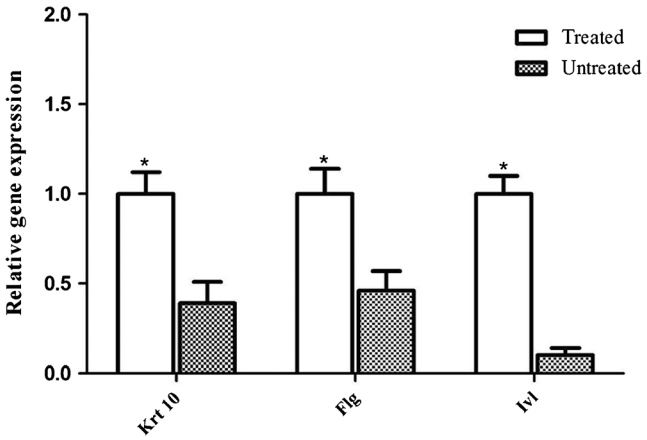

Fig. 4 Comparison of Krt 10, Flg, and Ivl expression levels between ADSCs, which were cultured on nanofibrous scaffolds in induction media (treated) and normal media (untreated) as the control. (*$P < 0.05$)

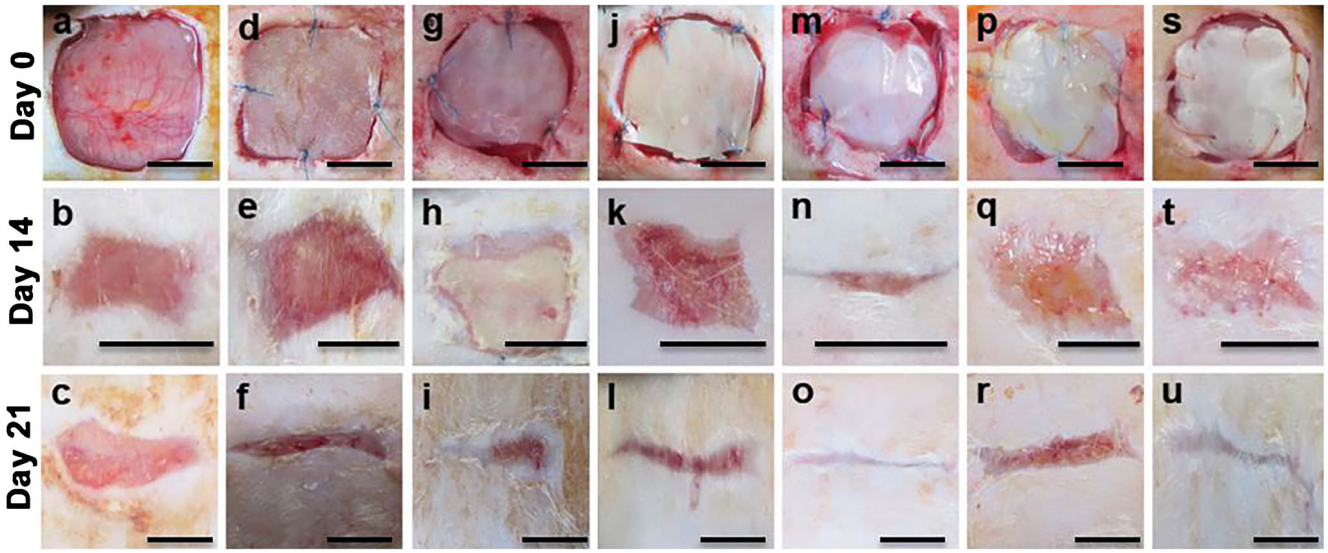

Fig. 5 Appearance of wound healing process in different groups on days 14 and 21 post-treatment. Control group (**a**–**c**), ADM group (**d**–**f**), ADM-ADSCs group (**g**–**i**), nanofiber group (**j**–**l**), nanofiber-ADSCs group (**m**–**o**), bilayer group (**p**–**r**), bilayer-ADSCs group (**s**–**u**). Scale bars represent 1 cm

Histomorphometric analysis

The histomorphometric analysis was conducted in order to assess the epithelialization, neovascularization, and the collagen density. Among all groups, re-epithelialization in ADM and control groups was minimum, and it was mostly filled with immature granulation tissue ($P < 0.05$). The best re-epithelialization was seen in bilayer and nanofiber scaffolds incorporated with ADSCs (the data is shown in Table 2). Wound healing process is heavily dependent on collagen synthesis. Therefore, to further investigate the effect of different treatments on wound healing, sections of animal skin tissues were stained with MT staining (Fig. 8). This staining was used to recognize the progress of collagen synthesis during granulation tissue formation and matrix remodeling. Collagen fibers were stained blue-green in MT staining method since the intensity of such a color corresponds to the relative amount of deposited total collagen and reflects the advancement of collagen synthesis and remodeling. The results indicated that among the experimental groups, ADSCs-seeded groups had the greatest collagen synthesis. The collagen density for nanofiber-ADSCs was obtained 87.4 ± 4.9%. In contrast, the rate of collagen fiber synthesis and deposition in wounds was the lowest in control group (8.3 ± 1.6%) and ADM group (35.8 ± 4.4%). The blood vessel density was evaluated by immunohistological staining of wound sections for the endothelial protein CD31 (Fig. 9). At day 14, the average blood vessel density for ADM-ADSCs, nanofiber-ADSCs, and bilayer-ADSCs were 79.5 ± 4.7, 92.7 ± 6.8, and 88.2 ± 5.9, respectively, which was significantly

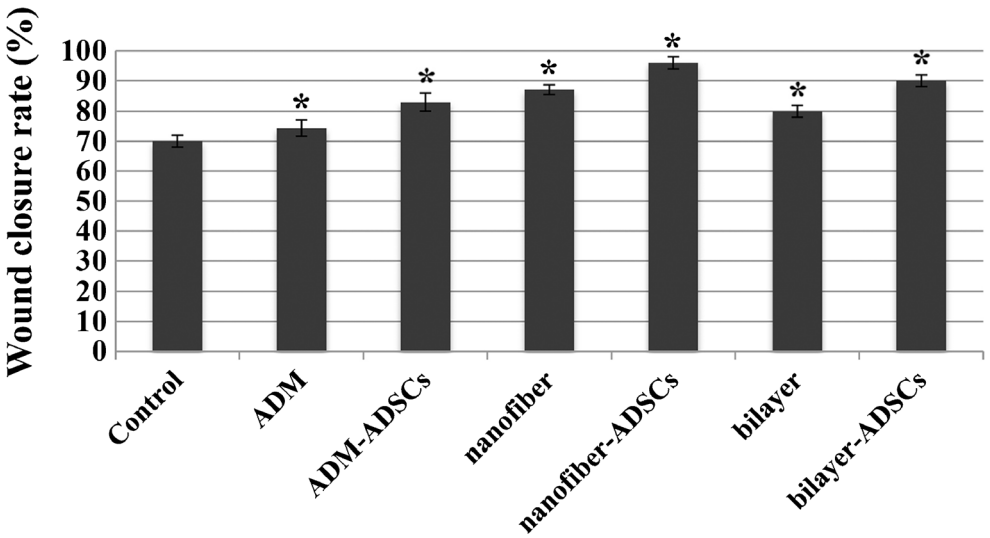

Fig. 6 Analysis of wound closure rates of different groups on the day 21. Data is presented as mean ± SD with $n = 4$ for each group. (*$P < 0.05$) versus control group

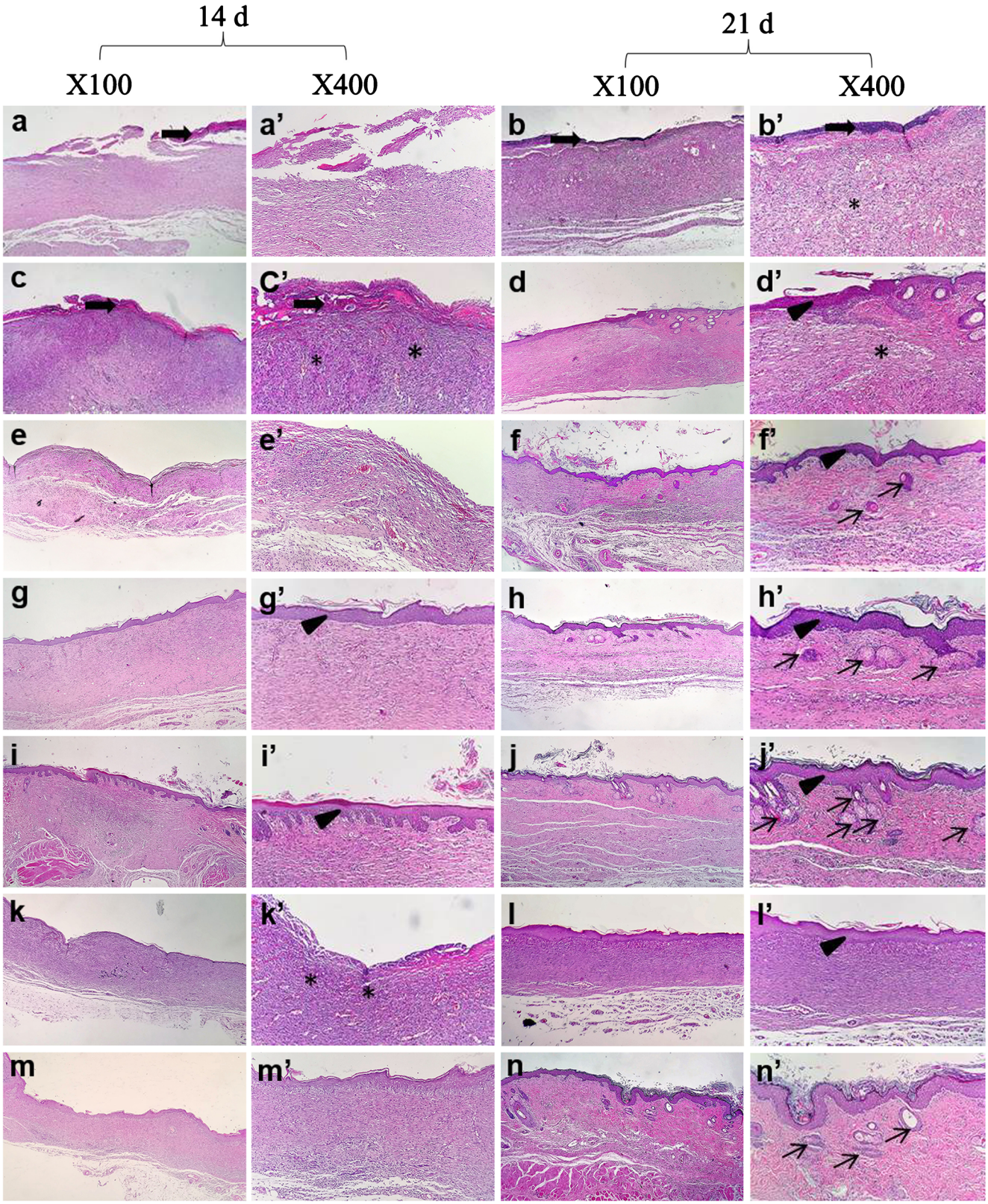

Fig. 7 H&E stained microscopic sections of healed incisions in the different treatment groups on days 14 and 21. Control group **a**–**b′**, ADM group **c**–**d′**, ADM-ADSCs group (**e**–**f′**), nanofiber group (**g**–**h′**), nanofiber-ADSCs group (**i**–**j′**), bilayer group (**k**–**l′**), bilayer-ADSCs group (**m**–**n′**). Thick arrows: crusty scab, thin arrows: rejuvenation of skin appendages, asteroid: accumulation of inflammatory cells, arrowhead: epidermal layer

Table 2 Epitheliogenesis scores of different experimental groups on the day 21 post-treatment

Group	Epitheliogenesis score ($N = 4$)
Control	1,0,0,0
ADM	2,0,2,1 *
ADM-ADSCs	3,3,2,3 **
nanofiber	3,4,4,2 ***
nanofiber-ADSCs	4,4,4,4 ***
bilayer	3,3,3,2 **
bilayer-ADSCs	4,4,4,3 ***

*, **, ***: values indicate treatment group versus un-treatment group (control)

*$P < 0.05$

**$P < 0.01$

***$P < 0.001$

higher in wounds treated with cell-free scaffold including ADM (40.3 ± 2.1), nanofiber (58.4 ± 4.5), bilayer (53.8 ± 3.6), and control (25.2 ± 3.4). The collagen density and average vessel density were summarized in Table 3.

Discussion

Nanofibers have been widely investigated in the area of skin tissue engineering. Nanofibers are attractive for wound healing applications due to the numerous inherent properties. The high surface area to volume ratio and microporous structure of the nanofibers provides cell adhesion, proliferation, and differentiation and also allows for fluid accumulation and oxygen permeability (Arasteh et al. 2016; Pilehvar-Soltanahmadi et al. 2016). Nanofibers from synthetic or natural polymers can be fabricated by electrospinning technique (Esnaashari et al. 2014). PCL, FAD approved polymer, has some properties such as biodegradability, biocompatibility, and appropriate mechanical properties. However, the in vivo application might limited due to hydrophobicity with no bioactive fragments (Bahrami et al. 2016; Karuppuswamy et al. 2015). In our previous study, it was shown that blending fibrinogen with PCL will improve the hydrophilicity and cytocompatibility of the PCL nanofibers. It has been reported that the hydrophilic surface would lead to higher cell adhesion than the hydrophobic surface (Meng et al. 2010). The results showed that ADSCs had a significant better proliferation rate on the blended scaffold

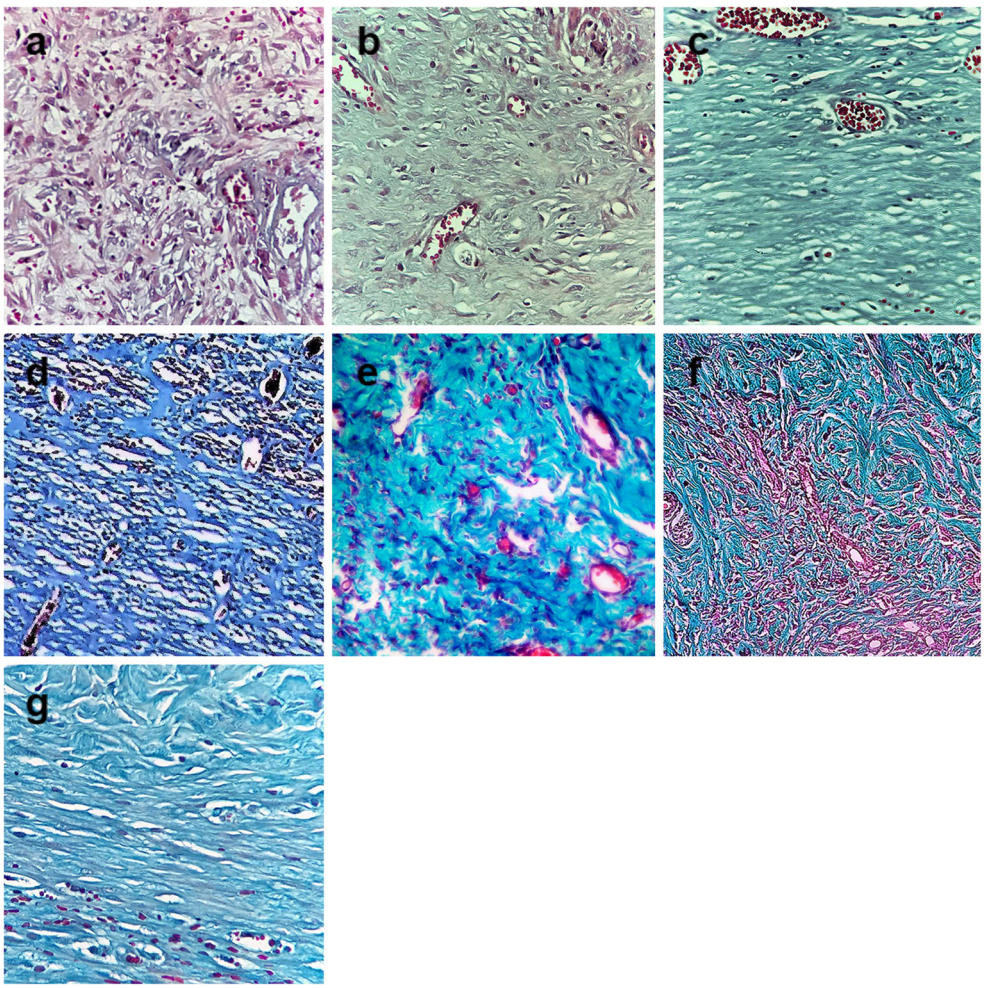

Fig. 8 MT stained microscopic sections of healed incisions in different groups on the day 21 post-treatment. **a** Control, **b** ADM, **c** ADM-ADSCs, **d** nanofiber, **e** nanofiber-ADSCs, **f** bilayer, **g** bilayer-ADSCs. All stained sections were visualized at magnification ×400

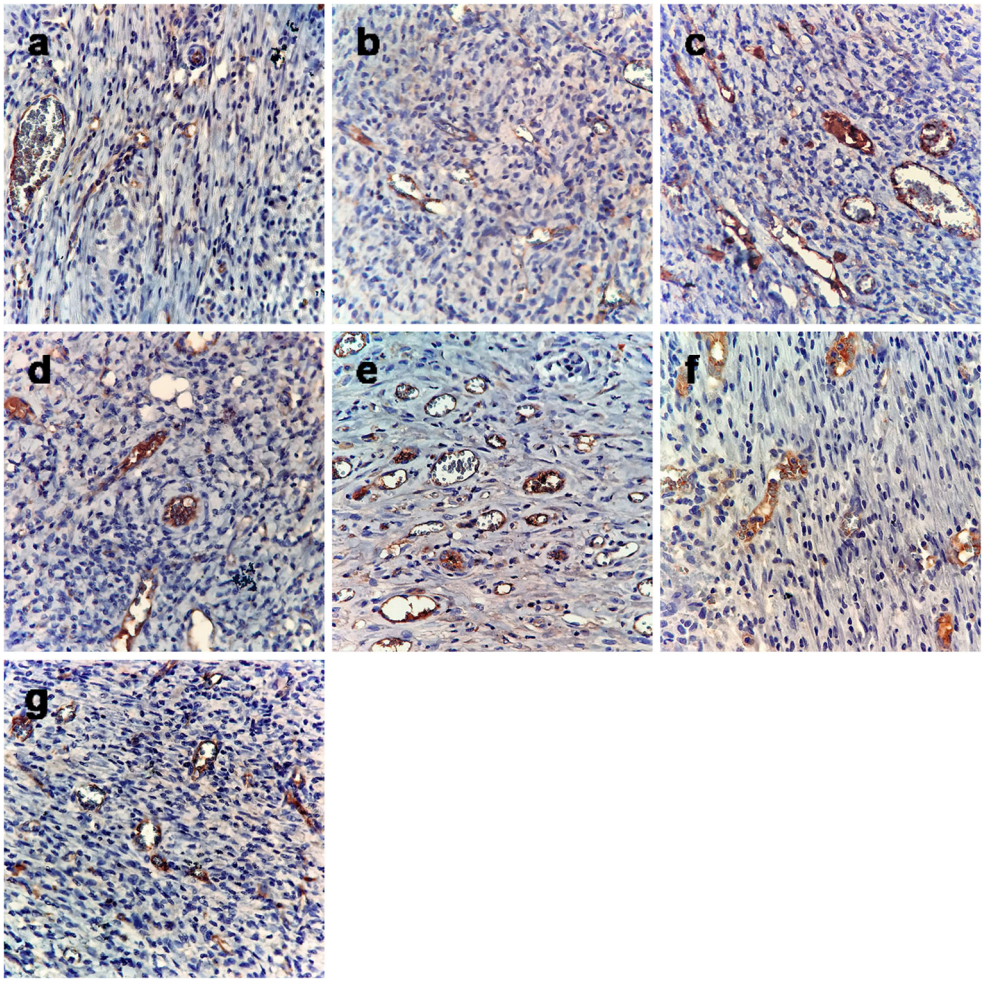

Fig. 9 Immunostaining of the healed incisions in different treatment groups for angiogenesis on the day 14 post-treatment. Immunohistochemical analysis of the CD31 genes was used to determine the angiogenesis in samples. The brown color represents positive staining for CD31. **a** Control, **b** ADM, **c** ADM-ADSCs, **d** nanofiber, **e** nanofiber-ADSCs, **f** bilayer, **g** bilayer-ADSCs. All stained sections were visualized at magnification ×400

compared to PCL scaffold. It has been shown that fibrinogen scaffolds support cell proliferation and promote cell interaction (Carlisle et al. 2009). MSCs can be isolated from bone marrow, cord blood, and adipose tissue. However, adipose tissue has a significantly higher stem cell density than bone marrow with several advantages including, lower donor morbidity, and relative abundance and also have higher proliferation potential in comparison to bone marrow stem cells (BMSC) (Jin et al. 2013; Ravichandran et al. 2013; Shokrgozar et al. 2012). Several studies have shown the capacity of ADSCs in epidermal differentiation using different medium inductions or different nanofiber substrates (Gaspar et al. 2016; Jin et al. 2013; Pilehvar-Soltanahmadi et al. 2017; Ravichandran et al. 2013; Shokrgozar et al. 2012). Younes Pilehvar et al. demonstrated that electrospun EO-PCL/PEG nanofibrous mat can act as a scaffold for differentiation of ADSCs to epidermal linage and suggest this scaffolds as a candidate for wound dressings and skin bioengineered substitutes with ADSCs (Pilehvar-Soltanahmadi et al. 2017). Rajeswari Ravichandran indicated that ADSCs can adhere, proliferate, and further differentiate into epidermal lineage on PVA/gelatin/azide nanofibers (Ravichandran et al. 2013). Guorui Jin et al. prepared blended and core-shell nanofibers containing epidermal induction factors (EIF) to evaluate the epidermal differentiation potential of ADSCs. They found that core-shell nanofibers have higher

Table 3 Number of blood vessels and collagen density of different experimental groups

Group	Blood vessels/5 HPF (×400) (14D)	Collagen density (%) (21D)
Control	25.2 ± 3.4	8.3 ± 1.6
ADM	40.3 ± 2.1*	35.8 ± 4.4*
ADM-ADSCs	79.5 ± 4.7***	63.4 ± 6.2**
Nanofiber	58.4 ± 4.5**	69.1 ± 3.4**
Nanofiber-ADSCs	92.7 ± 6.8***	87.4 ± 4.9***
Bilayer	53.8 ± 3.6**	51.0 ± 5.3*
Bilayer-ADSCs	88.2 ± 5.9***	74.5 ± 3.1***

*, **, ***: values indicate treatment group versus un-treatment group (control)

*$P < 0.05$

**$P < 0.01$

***$P < 0.001$

percentage of differentiation of ADSCs to epidermal lineages compared to blended nanofibers (Jin et al. 2013). In this study, ADSCs were differentiated to keratinocytes using new culture medium including KGF, EGF, insulin-transferrin-selenium (ITS), hydrocortisone, and L-ascorbic acid. ITS is cocktail which is extensively used in chondrocyte engineering. However, C. Mainzer et al. showed the ability of ITS medium to promote the expression of keratinocyte proliferation and differentiation markers (Mainzer et al. 2014). For cells differentiating toward epithelial lineage, keratin 10 is an early differentiation marker which is expressed in all suprabasal layers of the epidermis. Filaggrin and involucrin are intermediate and late epidermal differentiation makers, respectively. Filaggrin is expressed in well-differentiated keratinized epithelial cells, while involucrin is expressed in the upper spinous and granular layers of human skin (Jin et al. 2011; Pilehvar-Soltanahmadi et al. 2017). To confirm epidermal differentiation of ADSCs on nanofibrous scaffolds at the gene level, real-time PCR was performed to investigate the expression of Krt 10, Flg, and Ivl. The real-time PCR results showed a significant increase in expression of all three genes for ADSCs cultured on scaffold with induction medium compared to ADSCs cultured scaffolds in normal growth medium ($P < 0.05$). Skin wounds are divided into superficial, partial-thickness, or full-thickness wounds. Healing of full-thickness wound is more difficult than the superficial or partial-thickness wounds due to the lack of dermal tissue (Chen et al. 2017b; Guo et al. 2014). To optimize full-thickness wound repair, the development of an artificial dermis is necessary as a replacement to autografts (Wood et al. 2007). Numerous experiments have shown that ADM and nanofibrous scaffolds can be considered as a skin substitute. ADM, mostly obtained from human or animal skin dermal ECM, is inactivated immunologically by removing the epidermal and dermal cells. This scaffold has been recently used successfully to promote full-thickness cutaneous wound repair (Chen et al. 2017a; Sahin et al. 2014). ADM is resistant to infection, nonimmunogenic, and integrated rapidly into the recipient tissues (Orbay et al. 2011). Qiannan Wang et al. found that ADM-seeded MSCs has great potential as a scaffold for the treatment of full-thickness skin wounds. They realized that MSCs seeded ADM lead to promote neovascularization, ECM remodeling, and complete skin regeneration (Wang et al. 2015). Huang Sheng-Ping attempted to evaluate the synergic effects of ADSCs seeded on an ADM to treat full-thickness defects in a murine model. They revealed that seeding ADSC on ADM can enhance wound healing, promote angiogenesis, and increase the rate of re-epithelialization compared to the ADM (Huang et al. 2012). Ismail Sahin et al. improved the neo-vascularisation of ADM by using MSCs and negative pressure wound therapy (NPWT) simultaneously (Sahin et al. 2014). Kun Ma et al. used nanofibers as a carrier for local delivery of BMSC. They showed that nanofiber scaffolds with sufficient amount of BMSC can enhance healing of full-thickness skin wounds (Ma et al. 2011). Neovascularization is important for wound healing due to facilitating nutrient exchange and delivery of cells to the wound size (Yao et al. 2017). Almost all growth factors take part in normal wound healing, such as KGF, epidermal growth factor (EGF), vascular endothelial growth factor (VEGF), fibroblast growth factor-2 (FGF-2), hepatocyte growth factor (HGF), and platelet-derived growth factor secrete by ADSCs (Toyserkani et al. 2015). In this study, similar results were obtained. It was demonstrated that neovascularization and a large number of endothelial cells were present in wounds treated with bilayer-ADSCs, nanofiber-ADSCs, and ADM-ADSCs groups in comparison to the cell-free scaffolds and control group. Moreover, loaded ADSCs on nanofiber, ADM, and bilayer can enhance wound healing and re-epithelialization. There is a significant difference between nanofiber-ADSCs, bilayer-ADSCs with ADM-ADSCs ($P < 0.05$), and also a significant difference was found between ADM and nanofibers ($P < 0.01$) in the rate of re-epithelialization or wound healing. On the basis of these results, there is no significant difference between nanofiber-ADSCs and bilayer-ADSCs; however, the nanofiber-ADSCs showed the best results. This can be attributed to the role of nanofibers in accelerated wound healing. Paul P. Bonvallet suggested that microporous electrospun scaffolds are effective substrates for skin regeneration (Bonvallet et al. 2014).

Conclusion

In the current study, nanofibers have been developed and evaluated for their potential to support proliferation and differentiation of ADSCs to epidermal lineage. Real-time PCR confirmed the expression of epidermal markers of Krt 10, Flg, and Ivl. To our knowledge, there is no study evaluating the effectiveness of nanofiber-ADM containing ADSCs in the closure of full-thickness wound by a single-step procedure. Further investigations are needed in order to optimize this technique to produce bilayer scaffolds as an alternative for split-thickness grafts. This study revealed that ADSCs seeded onto ADM, nanofiber, and bilayer scaffolds can promote regeneration, re-epithelialization, angiogenesis, and collagen remodeling in comparison to the cell-free scaffolds and control. Also, ADM can be integrated into wound bed or enhanced wound healing when covered with nanofibers or seeded with ADSCs. However, the nanofiber-ADSCs have the best cosmetic appearance with a normal thickness of epidermal layer and rejuvenation of the hair follicles and skin appendages and have the potential to be a suitable dressing for treatment of full-thickness skin wounds.

Funding information This project was supported by the Tehran University of Medical Sciences (TUMS), (grant No. 94-0287-28594).

Compliance with ethical standards

Conflict of interest The authors have no conflicts of interest.

Ethical approval All applicable international, national, and/or institutional guidelines for the care and use of animals were followed.

References

Arasteh S, Kazemnejad S, Khanjani S, Heidari-Vala H, Akhondi MM, Mobini S (2016) Fabrication and characterization of nano-fibrous bilayer composite for skin regeneration application. Methods 99:3–12

Bahrami H, Keshel SH, Chari AJ, Biazar E (2016) Human unrestricted somatic stem cells loaded in nanofibrous PCL scaffold and their healing effect on skin defects. Artif Cells Nanomed Biotechnol 44(6):1556–1560

Bonvallet PP, Culpepper BK, Bain JL, Schultz MJ, Thomas SJ, Bellis SL (2014) Microporous dermal-like electrospun scaffolds promote accelerated skin regeneration. Tissue Eng A 20(17–18):2434–2445

Carlisle CR, Coulais C, Namboothiry M, Carroll DL, Hantgan RR, Guthold M (2009) The mechanical properties of individual, electrospun fibrinogen fibers. Biomaterials 30(6):1205–1213

Chen M, Jin Y, Han X, Wang N, Deng X, Liu H (2017a) MSCs on an acellular dermal matrix (ADM) sourced from neonatal mouse skin regulate collagen reconstruction of granulation tissue during adult cutaneous wound healing. RSC Adv 7(37):22998–23010

Chen S, Liu B, Carlson MA, Gombart AF, Reilly DA, Xie J (2017b) Recent advances in electrospun nanofibers for wound healing. Nanomedicine 12(11):1335–1352

Demiri E, Papaconstantinou A, Dionyssiou D, Dionyssopoulos A, Kaidoglou K, Efstratiou I (2013) Reconstruction of skin avulsion injuries of the upper extremity with integra® dermal regeneration template and skin grafts in a single-stage procedure. Arch Orthop Trauma Surg 133(11):1521–1526

Esnaashari SS, Rezaei S, Mirzaei E, Afshari H, Rezayat SM, Faridi-Majidi R (2014) Preparation and characterization of kefiran electrospun nanofibers. Int J Biol Macromol 70:50–56

Foubert P, Barillas S, Gonzalez AD, Alfonso Z, Zhao S, Hakim I, Meschter C, Tenenhaus M, Fraser JK (2015) Uncultured adipose-derived regenerative cells (ADRCs) seeded in collagen scaffold improves dermal regeneration, enhancing early vascularization and structural organization following thermal burns. Burns 41(7):1504–1516

Gaspar A, Constantin D, Seciu A-M, Moldovan L, Craciunescu O, Ganea E (2016) Human adipose-derived stem cells differentiation into epidermal cells and interaction with human keratinocytes in coculture. Turk J Biol 40(5):1111–1120

Guo R, Teng J, Xu S, Ma L, Huang A, Gao C (2014) Comparison studies of the in vivo treatment of full-thickness excisional wounds and burns by an artificial bilayer dermal equivalent and J-1 acellular dermal matrix. Wound Repair Regen 22(3):390–398

Haslik W, Kamolz L-P, Manna F, Hladik M, Rath T, Frey M (2010) Management of full-thickness skin defects in the hand and wrist region: first long-term experiences with the dermal matrix Matriderm®. J Plast Reconstr Aesthet Surg 63(2):360–364

Hosseinzadeh S, Soleimani M, Vossoughi M, Ranjbarvan P, Hamedi S, Zamanlui S, Mahmoudifard M (2017) Study of epithelial differentiation and protein expression of keratinocyte-mesenchyme stem cell co-cultivation on electrospun nylon/B. vulgaris extract composite scaffold. Mater Sci Eng C 75:653–662

Huang S-P, Hsu C-C, Chang S-C, Wang C-H, Deng S-C, Dai N-T, Chen T-M, Chan JY-H, Chen S-G, Huang S-M (2012) Adipose-derived stem cells seeded on acellular dermal matrix grafts enhance wound healing in a murine model of a full-thickness defect. Ann Plast Surg 69(6):656–662

Jin G, Prabhakaran MP, Kai D, Ramakrishna S (2013) Controlled release of multiple epidermal induction factors through core–shell nanofibers for skin regeneration. Eur J Pharm Biopharm 85(3):689–698

Jin G, Prabhakaran MP, Ramakrishna S (2011) Stem cell differentiation to epidermal lineages on electrospun nanofibrous substrates for skin tissue engineering. Acta Biomater 7(8):3113–3122

Karuppuswamy P, Venugopal JR, Navaneethan B, Laiva AL, Ramakrishna S (2015) Polycaprolactone nanofibers for the controlled release of tetracycline hydrochloride. Mater Lett 141:180–186

Ma K, Liao S, He L, Lu J, Ramakrishna S, Chan CK (2011) Effects of nanofiber/stem cell composite on wound healing in acute full-thickness skin wounds. Tissue Eng A 17(9–10):1413–1424

Mainzer C, Barrichello C, Debret R, Remoué N, Sigaudo-Roussel D, Sommer P (2014) Insulin–transferrin–selenium as an alternative to foetal serum for epidermal equivalents. Int J Cosmet Sci 36(5):427–435

Meng Z, Wang Y, Ma C, Zheng W, Li L, Zheng Y (2010) Electrospinning of PLGA/gelatin randomly-oriented and aligned nanofibers as potential scaffold in tissue engineering. Mater Sci Eng C 30(8):1204–1210

Mirzaei E, Ai J, Ebrahimi-Barough S, Verdi J, Ghanbari H, Faridi-Majidi R (2016) The differentiation of human endometrial stem cells into neuron-like cells on electrospun PAN-derived carbon nanofibers with random and aligned topographies. Mol Neurobiol 53(7):4798–4808

Orbay H, Takami Y, Hyakusoku H, Mizuno H (2011) Acellular dermal matrix seeded with adipose-derived stem cells as a subcutaneous implant. Aesthet Plast Surg 35(5):756

Philandrianos C, Andrac-Meyer L, Mordon S, Feuerstein J-M, Sabatier F, Veran J, Magalon G, Casanova D (2012) Comparison of five dermal substitutes in full-thickness skin wound healing in a porcine model. Burns 38(6):820–829

Pilehvar-Soltanahmadi Y, Akbarzadeh A, Moazzez-Lalaklo N, Zarghami N (2016) An update on clinical applications of electrospun nanofibers for skin bioengineering. Artif Cells Nanomed Biotechnol 44(6):1350–1364

Pilehvar-Soltanahmadi Y, Nouri M, Martino MM, Fattahi A, Alizadeh E, Darabi M, Rahmati-Yamchi M, Zarghami N (2017) Cytoprotection, proliferation and epidermal differentiation of adipose tissue-derived stem cells on emu oil based electrospun nanofibrous mat. Exp Cell Res 357(2):192–201

Ravichandran R, Venugopal JR, Sundarrajan S, Mukherjee S, Forsythe J, Ramakrishna S (2013) Click chemistry approach for fabricating PVA/gelatin nanofibers for the differentiation of ADSCs to keratinocytes. J Mater Sci Mater Med 24(12):2863–2871

Ryssel H, Gazyakan E, Germann G, Öhlbauer M (2008) The use of MatriDerm® in early excision and simultaneous autologous skin grafting in burns—a pilot study. Burns 34(1):93–97

Sahin I, Ozturk S, Deveci M, Ural AU, Onguru O, Isik S (2014) Experimental assessment of the neo-vascularisation of acellular dermal matrix in the wound bed pretreated with mesenchymal stem cell under subatmospheric pressure. J Plast Reconstr Aesthet Surg 67(1):107–114

Shokrgozar MA, Fattahi M, Bonakdar S, Kashani IR, Majidi M, Haghighipour N, Bayati V, Sanati H, Saeedi SN (2012) Healing potential of mesenchymal stem cells cultured on a collagen-based scaffold for skin regeneration. Iran Biomed J 16(2):68

Soejima K, Chen X, Nozaki M, Hori K, Sakurai H, Takeuchi M (2006) Novel application method of artificial dermis: one-step grafting procedure of artificial dermis and skin, rat experimental study. Burns 32(3):312–318

Sundaramurthi D, Krishnan UM, Sethuraman S (2014) Epidermal differentiation of stem cells on poly (3-hydroxybutyrate-co-3-hydroxyvalerate)(PHBV) nanofibers. Ann Biomed Eng 42(12): 2589–2599

Toyserkani NM, Christensen ML, Sheikh SP, Sørensen JA (2015) Adipose-derived stem cells: new treatment for wound healing? Ann Plast Surg 75(1):117–123

Wang Q, Jin Y, Deng X, Liu H, Pang H, Shi P, Zhan Z (2015) Second-harmonic generation microscopy for assessment of mesenchymal stem cell-seeded acellular dermal matrix in wound-healing. Biomaterials 53:659–668

Wang X, You C, Hu X, Zheng Y, Li Q, Feng Z, Sun H, Gao C, Han C (2013) The roles of knitted mesh-reinforced collagen–chitosan hybrid scaffold in the one-step repair of full-thickness skin defects in rats. Acta Biomater 9(8):7822–7832

Wood FM, Stoner ML, Fowler BV, Fear MW (2007) The use of a non-cultured autologous cell suspension and Integra® dermal regeneration template to repair full-thickness skin wounds in a porcine model: a one-step process. Burns 33(6):693–700

Xu Y, Liu Z, Liu L, Zhao C, Xiong F, Zhou C, Li Y, Shan Y, Peng F, Zhang C (2008) Neurospheres from rat adipose-derived stem cells could be induced into functional Schwann cell-like cells in vitro. BMC Neurosci 9(1):21

Yao C-H, Lee C-Y, Huang C-H, Chen Y-S, Chen K-Y (2017) Novel bilayer wound dressing based on electrospun gelatin/keratin nanofibrous mats for skin wound repair. Mater Sci Eng C 79:533–540